

# Numerical Study for Clarifying Scale Effects on Flow and Heat Transfer Characteristics Around an Isolated Building

Yezhan Li <sup>a</sup>, Kyoshiro Masuda <sup>b</sup>, Naoki Ikegaya <sup>c</sup>

<sup>a</sup>*Faculty of Engineering Sciences, Kyushu University, Fukuoka, Japan, li.yezhan.628@m.kyushu-u.ac.jp*

<sup>b</sup>*Interdisciplinary Graduate School of Engineering Sciences, Kyushu University, Fukuoka, Japan, masuda.kyoshiro.181@s.kyushu-u.ac.jp*

<sup>c</sup>*Faculty of Engineering Sciences, Kyushu University, Fukuoka, Japan, ikegaya.naoki.116@m.kyushu-u.ac.jp*

## SUMMARY

The characterization of momentum and scalar exchange around buildings is critical for urban environmental studies. The Reynolds number ( $Re$ ) dependence of a scalar transport process remains, known as a scale effect, poorly quantified especially for specific surfaces of an isolated building, whereas momentum transport can easily achieve a fully rough condition where both the velocity field and momentum exchange do not depend on  $Re$ . Therefore, this study systematically investigates the  $Re$  effects on local heat transfer using large-eddy simulation and Reynolds-averaged Navier–Stokes turbulence models. Momentum transport becomes  $Re$ -independent beyond  $Re \geq 1.5 \times 10^4$ , while thermal transport remains sensitive for  $Re < 1.5 \times 10^6$ . In addition, the Stanton number decreases with  $Re$ , whereas the Nusselt number increases following a power-law relationship. They never reach to a  $Re$ -independent condition, although the drag coefficient is dominated by pressure drag rather than ground-surface friction. These findings highlight the need to consider  $Re$ -dependence in urban-scale simulations.

**Keywords:** *Reynolds number, Heat transfer, Stanton number, Nusselt number, Drag coefficient*

## 1. INTRODUCTION

Understanding how momentum and scalars are exchanged between buildings surfaces and surrounding airflows is essential for urban microclimate prediction and pollutant dispersion modeling. Most existing studies have focused on the turbulent characteristics around the buildings at a specific Reynolds number ( $Re$ ) regardless of full or model scale by relying on the fact the airflow is independent on  $Re$  above its critical value. However, concerning  $Re$ -dependency of scalar transfer, scalar exchange coefficients may still exhibit dependence on  $Re$  even at very high roughness as Ikegaya et al. (Ikegaya et al. 2020) pointed out in their study on scalar transport over cubic arrays. This is because of the difference in the net source/sink production mechanisms for the momentum and scalar. That is, scalar source is governed solely by the molecular diffusion on surfaces, whereas momentum sink dominantly occurred by the pressure drag. Although these qualitative processes been well known, for an isolated building, especially under varying Reynolds numbers, the local contribution mechanisms of different surfaces (e.g., windward, leeward) to momentum and heat exchange have not yet been sufficiently elucidated. Consequently, two notable gaps remain in current research: first, an insufficient understanding of how aerodynamic and thermal characteristics vary across a broad range of  $Re$ ; second, a lack of systematic quantification of the  $Re$ -dependence of local surface-specific dimensionless numbers, such as Stanton number ( $St$ ), Nusselt number ( $Nu$ ), and drag coefficient ( $Cd$ ).

To systematically investigate this scale effect, this study employs one large-eddy simulation (LES) and three Reynolds-averaged Navier–Stokes (RANS) turbulence models, including standard  $k - \varepsilon$  model, realizable  $k - \varepsilon$  model, and RNG model, to simulate the flow field around an isolated

building. By systematically varying  $Re$ , the research examines the variation of  $St$  and  $Nu$  across different building surfaces, including windward, leeward, top, and ground surfaces, as well as the  $Cd$  of the entire building and ground areas.

## 2. METHOD

### 2.1. Numerical Setting

As shown in Figure 1(a), the computational domain replicates the geometric setup in a wind-tunnel experiment (WTE), Case-J (AIJ benchmark, 2020), published by the Architectural Institute of Japan (AIJ). The building is represented as a rectangular block with a height  $H = 0.16$  m and a width  $D = 0.08$  m. The extent of the domain spans  $12.5H$ ,  $7.5H$ , and  $6.25H$  in the streamwise, lateral, and vertical directions, respectively. The corresponding coordinates and velocity components are denoted as  $x$ ,  $y$ ,  $z$  and  $u$ ,  $v$ ,  $w$ . The mesh arrangement is illustrated in Figure 1(b). The grid comprises 40 layers in the vertical direction, 20 cells along each lateral face, and 28 divisions on both the windward and leeward surfaces of the building. The entire computational mesh contains approximately 1.49 million hexahedral cells. To ensure a consistent basis for model comparison, the identical mesh configuration was utilized for the LES and all three RANS simulations.

Both LES and RANS simulations employ largely consistent boundary conditions, with two key exceptions applied to the inlet and the lateral and top boundaries to accommodate their respective methodologies. At the inlet, the LES utilizes a fully turbulent inflow containing velocity and temperature fluctuations generated by the precursor method. In contrast, the three RANS models adopt the mean velocity and temperature profiles from the referenced WTE (as shown in Figure 1(c).  $u_H$  and  $T_f$  represent the velocity at the building height and the floor temperature.  $\Delta T = T_f - T_H$ , where  $T_H$  is the temperature at the building height.) as their inflow condition, supplemented with corresponding profiles for turbulent kinetic energy (TKE) and its dissipation rate ( $\varepsilon$ ). Regarding the lateral and top boundaries, a no-slip condition is applied in the LES, while a free-slip condition is specified for the RANS cases. All other boundaries are identical across both frameworks. A zero-gradient condition is enforced at the downstream outlet. The Spalding wall function is implemented for momentum, and the Jayatilleke wall function is applied for thermal transport. Both the building surfaces and the ground are heated to a constant temperature of  $45.8$  °C.

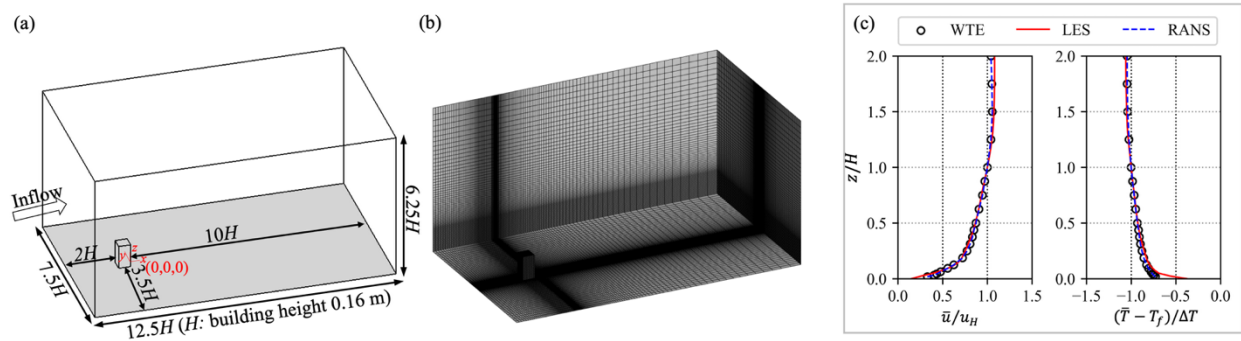


Figure 1: (a) computational domain, (b) mesh arrangement, and (c) inflow profiles of mean velocity and mean temperature at the vertical plane  $y/H = 0$ .

## 2.2. Validation

Figure 2 compares the profiles of mean streamwise velocity component, TKE, and mean temperature at the vertical plane ( $y/H = 0$ ) for LES, three RANS models, and the WTE results. All RANS models underestimate the velocity and TKE but overestimate the mean temperature in the recirculation zone of the wake. This discrepancy originates from the fundamental closure problem of the RANS methodology, wherein the time-averaging procedure inherently dissipates the energetic, large-scale unsteady characteristic of separating flows. Among the RANS models, the RNG  $k - \varepsilon$  model shows the best agreement due to its theoretically derived constants and an additional term in its  $\varepsilon$ -equation that improves response to rapid strain and streamline curvature. Consequently, the RNG  $k - \varepsilon$  model is selected for subsequent analysis of Reynolds number effects.

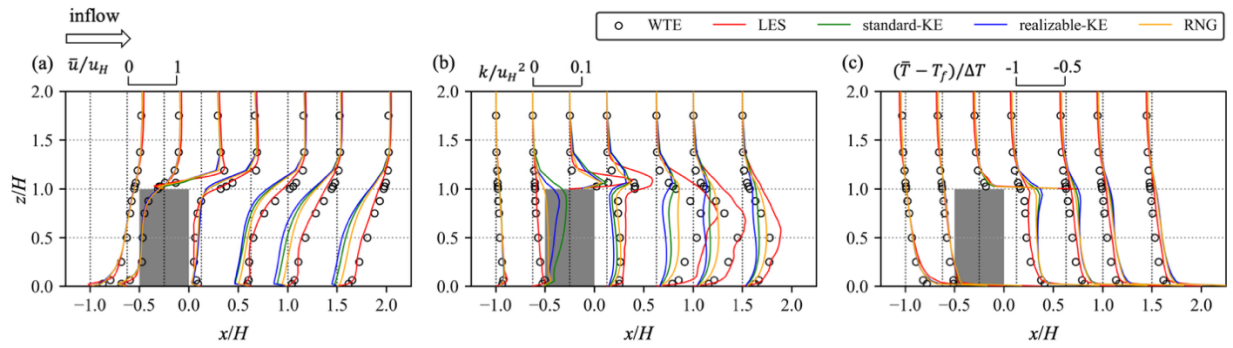


Figure 2: Profiles of (a) mean streamwise velocity, (b) TKE, and (c) mean temperature at plane  $y/H = 0$  for cases with different turbulent models.

## 3. RESULTS&DISCUSSION

Figure 3 compares the profiles of mean streamwise velocity component, TKE, and mean temperature at the vertical plane ( $y/H = 0$ ) for different  $Re$  using the RNG model. For velocity and TKE profiles, only the case at the lowest  $Re$  ( $1.5 \times 10^3$ ) shows underestimation, while other cases show similar results, indicating that the momentum transport becomes  $Re$ -independent beyond this threshold  $Re \geq 1.5 \times 10^4$ . In contrast, the temperature profiles exhibit significant sensitivity across a much wider  $Re$  range. The thermal field remains strongly  $Re$ -dependent for  $Re < 1.5 \times 10^6$ . This delayed convergence stems from the fact that at lower  $Re$ , enhanced molecular diffusion increases the wall heat flux, leading to higher wake temperatures.

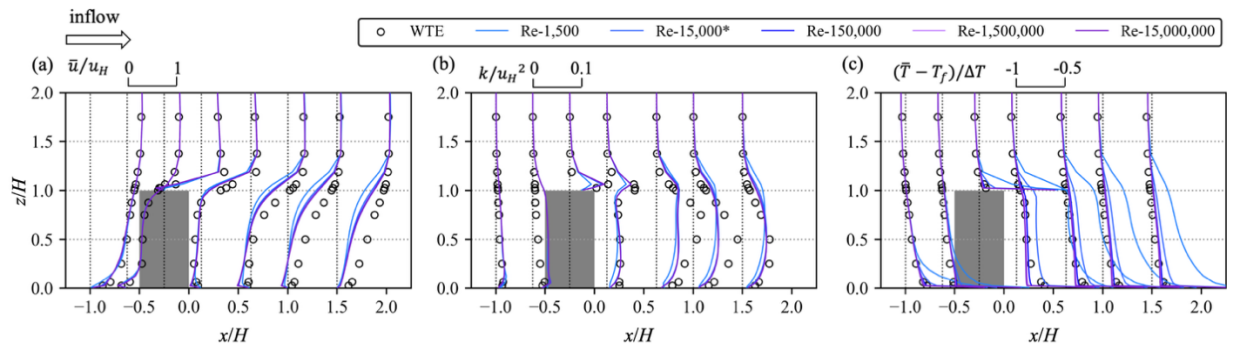


Figure 3: Profiles of (a) mean streamwise velocity, (b) TKE, and (c) mean temperature at plane  $y/H = 0$  for cases with different Reynolds number.

Figure 4 presents the dependence of  $St$ ,  $Nu$ , and  $Cd$  on the  $Re$  obtained from simulations using the RNG turbulence model. The three dimensionless parameters are defined as  $St = h/\rho C_p u$ ,  $Nu = hd/\rho C_p \alpha$ , and  $Cd = \tau/\rho u^2$ , respectively. Here,  $h$  is the convective heat transfer coefficient,  $\rho$  is the fluid density,  $C_p$  is the specific heat capacity at constant pressure,  $u$  is the characteristic velocity,  $d$  is the characteristic length scale,  $\alpha$  is the thermal diffusivity, and  $\tau$  is the wall shear stress. In Figure 4(a), the  $St$  for all surfaces decreases with increasing  $Re$  (Note that the  $St$  is shown in a linear axis. See Figure 4(b) for the power-law relationship since  $St = Nu/RePr$ , where  $Pr$  is the Prantdl number  $\alpha/\nu$ ). Notably, the overall  $St$  result closely follows that of the ground surface, indicating that the ground contribution dominates the overall  $St$  of the entire system. Figure 4(b) reveals that the  $Nu$  values for all surfaces increase significantly with increasing  $Re$ , displaying a typical power-law relationship expressed as  $Nu \propto Re^m$ . Figure 4(c) illustrates the contributions from pressure drag and viscous drag to the  $Cd$ . Both the total  $Cd$  and the viscous drag decrease continuously with increasing  $Re$ , while the pressure drag remains relatively constant across different  $Re$  values. This indicates that the overall drag coefficient is predominantly governed by form drag rather than by the viscous drag.

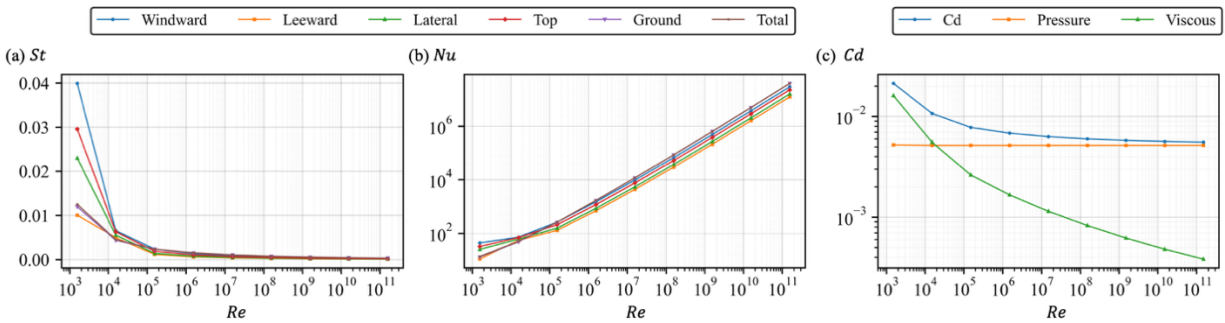


Figure 4: Relation between Reynolds number and (a) Stanton number, (b)Nusselt number, and (c) Drag coefficient.

## 4. CONCLUSIONS

This study systematically investigated the  $Re$ -dependence of momentum and scalar transport around an isolated building using numerical simulations. The results demonstrate that the  $St$  decreases with increasing  $Re$ , with the windward surface showing the most rapid decrease, and accordingly the  $Nu$  follows a typical power-law relationship. In contrast, the  $Cd$  is predominantly governed by the form drag. These findings provide valuable insights into the scaling behavior of building aerodynamics and heat transfer, highlighting the need to account for  $Re$  effects in urban environmental simulations.

## ACKNOWLEDGEMENTS

Funding: This study was partially supported by the Grant-in-Aid for Scientific Research from JSPS KAKENHI (Grant Nos. JP23K26263, JP23K17789) and the FOREST program from JST (Grant No. JPMJFR205O).

## REFERENCES

- Ikegaya, N., 2020. Geometric and scale dependency of scalar transfer coefficient, Mesoscale & Microscale Meteorology Seminar Series, National Center for Atmospheric Research  
 AIJ benchmark, 2020. 1:1:2 shape building model with dispersion in non-isothermal flow. [https://www.aij.or.jp/jpn/publish/cfdguide/index\\_e.htm](https://www.aij.or.jp/jpn/publish/cfdguide/index_e.htm)